

Nanometer Scale Complementary Silicon MOSFETs as Detectors of Terahertz and Sub-terahertz Radiation

W. Stillman^{1,2} (stillw@rpi.edu), F. Guarin², V. Yu. Kachorovskii^{1,3}, N. Pala^{1,4}, S. Rumyantsev^{1,3},
M.S. Shur¹ and D. Veksler¹

1. Center for Integrated Electronics, Rensselaer Polytechnic Institute, Troy, NY 12180, USA. 2. IBM Microelectronics, 2070 Route 52, Hopewell Junction, NY 12533, USA. 3. Ioffe Institute of Russian Academy of Sciences, 194021 St. Petersburg, Russia. 4. Sensor Electronic Technology, Inc., 1195 Atlas Road, Columbia SC 29209, USA.

Abstract—We demonstrate, for the first time, THz detection by Si CMOS, i.e. by both p-channel and n-channel Si MOS devices. Previous work demonstrated that Si n-MOS devices detect THz and sub-THz radiation via the excitation of plasma waves in the device channel, with responsivity and Noise Equivalent Power on the order of commercial pyroelectric detectors but capable of operating at much greater speed as shown by a theory of temporal response predicting the maximum operating frequency. The CMOS responsivity is a strong increasing function of the drain current. Our experimental data and modeling results allow us to understand the effects of device geometry and bias on the Si CMOS THz detector performance.

I. INTRODUCTION

Terahertz sensing requires detectors possessing high responsivity, detectivity and fast response. In addition operation at room temperature or higher is now very frequently required. Among present devices used for terahertz detection at room temperature are pyroelectrics, Schottky diodes, High Electron Mobility Transistors (HEMTs) and silicon Field Effect Transistors (FETs). We now demonstrate, for the first time, that both p-channel and n-channel silicon MOSFETs can be used as efficient detectors of sub-THz and THz radiation and present data on the sub-THz response of nanometer gate silicon CMOS. A major advantage of these detectors over commercial pyroelectric devices is their extremely fast response, and we utilize a theory of temporal response that predicts the maximum operating frequency at zero drain bias to be on the order of $\mu V_{gt}/L^2$, and $\mu V_{th}/L^2$ for FETs operating above and below threshold, respectively. Here μ is the electron field effect mobility, V_{gt} is the gate voltage swing, $V_{th} = k_B T/q$ is the thermal voltage and L is the gate length. Using device parameters extracted from measured current-voltage characteristics, response to THz radiation as a function of the gate bias and detector load resistance is simulated. We show that the point of maximum detectivity corresponds to the device threshold voltage in open drain configurations. In addition, we discuss the enhancement of device response by the application of drain current and the implications to detectivity.

Devices used in our experiments were supplied by IBM Microelectronics, from the technology described by Steegen et al.[1] Regular Vt, Low Vt and High Vt (where Vt is the threshold voltage) devices were provided, with gate widths ranging from 1 μ m to 5 μ m, physical oxide thickness $t_{ox} \sim 2.0$ nm, and drawn gate lengths ranging from 50 nm to 180 nm.

II. TERAHERTZ RESPONSE

In 1993, Dyakonov and Shur predicted an instability of electron plasma waves in a short channel ballistic FET at terahertz frequencies.[2] With asymmetrically connected device terminals in short devices relative to the plasmon decay length, i.e. when $L \ll s \sqrt{\tau/\omega}$, these waves are amplified by reflections and result in a gate bias dependent resonant voltage response at the drain terminal. Here L is the device channel length, s is the wave velocity, τ is the momentum relaxation time and ω is the angular plasma wave frequency. Plasma waves couple to and can be excited by electromagnetic radiation, and, therefore, short channel FETs can be used as resonant THz detectors.[2] In sufficiently long devices however, i.e. when $L \gg s \sqrt{\tau/\omega}$, the oscillations are damped along the channel before reaching the drain terminal, and a non-resonant DC voltage related to the gate bias results. This response has been demonstrated in High Electron Mobility Transistors (HEMTs),[3] in submicron and nanoscale silicon MOSFETs[4, 5] and in Silicon on Insulator (SOI) MOSFETs[6]. These devices provide both broadband terahertz detection (but to a certain extent tunable by the gate bias) and fast response time. In addition, silicon and SOI MOSFETs also enjoy the advantage of being easily integrated into the large existing base of semiconductor fabrication, enabling detectors and signal processing elements to be combined.

A. Non-resonant response model

Dyakonov and Shur considered the case of gate bias above the device threshold in 1996[7]. This was expanded upon by Knap et al.,[3] to include the sub-threshold region by accounting for the exponential dependence of the electron concentration upon gate bias and gate leakage current. In our recent pub-

lication, we demonstrated the effects of loading and channel resistance on the response in the sub-threshold region.[8] In the case where gate leakage is sufficiently small so as to be neglected, non-resonant response is defined by the following expression[3, 8]:

$$\Delta v = \frac{1}{1 + R_{ch}/R_l} \left[\frac{qv_a}{4ms^2} \left(\frac{\sinh^2(Q) - \sin^2(Q)}{\sinh^2(Q) + \cos^2(Q)} \right) \right] \quad (1)$$

Here v_a is the small AC voltage appearing between the source and gate terminals as a result of the incoming radiation, m is the electron effective mass, $V_{gt} = V_{gs} - V_t$ is the gate to channel voltage swing and R_{ch} and R_l are the channel and load resistances, respectively. The parameter s is the plasma wave velocity described by[3]:

$$s^2 = s_0^2 \left[1 + \exp\left(-\frac{qV_{gt}}{\eta k_B T}\right) \right] \ln \left[1 + \exp\left(\frac{qV_{gt}}{\eta k_B T}\right) \right] \quad (2)$$

where $s_0 = (\eta k_B T/m)^{1/2}$ is the electron thermal velocity.

The parameter Q relates the frequency of the incoming radiation ω to the device momentum relaxation time τ , the channel length and the wave velocity as:

$$Q = \frac{L}{s} \sqrt{\omega/2\tau} \quad (3)$$

In general, the response modeled by Equation 1 is constant for $V_{gt} \ll 0$ and decreases as $1/V_{gt}$ for $V_{gt} \gg 0$. The trigonometric terms additionally diminish the response when $V_{gt} > 0$, but for $Q \geq 3$, have minimal effect. In order to model the response, device parameters were extracted from current / voltage measurements and verified using AIM Spice.

B. Open drain measurements

Sources at 0.2 and 0.6 THz consisted of a Gunn diode oscillator coupled to signal multipliers; the output power of these sources was 3mW and 80μW, respectively. The sub-terahertz beams were focused onto the detection device using a parabolic mirror after passing through an optical chopper. The 1.6 THz source was a CO₂ pumped far-infrared gas laser with a reported power of 180mW. Response measurements were made using a standard lock-in technique. The source terminal was grounded while gate voltage was swept through the range of device operation. A low noise preamplifier was connected between the device drain and the lock-in amplifier.

Fig. 1 (top) shows 0.2 THz response of length scaled RVt NFETs superimposed upon model values calculated from Eq. 1. Though the slope near the device threshold is substantially steeper in the model, in the sub-threshold region the model predicts well the observed response roll-off, clearly indicating

that for a given device width, loaded response is degraded by the increased resistance of longer device channels.

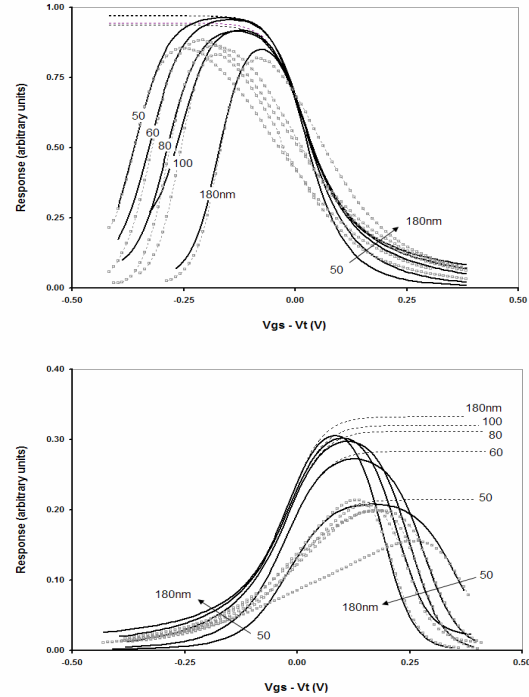


Figure 1. Measured (squares) and calculated 0.2 THz drain response of 2μm x L_{des} RVt NFETs (top) and RVt PFETs (bottom). Unloaded response (dashed lines) and response with an 8.2Mohm preamplifier input impedance load (heavy solid lines) are calculated using Eq. 1 with $m=0.19m_e$ and $\tau=0.005ps$ for NFETs and $m=0.54m_e$ and $\tau=0.007ps$ for PFETs.

Fig. 1 (bottom) shows 0.2 THz response for length scaled RVt PFETs. The PFET response is significantly lower than that of the NFETs, due to the larger effective mass of the holes compared with the electrons which reduces the (unloaded) maximum response, and to the larger channel resistance of the PFETs, which brings about earlier roll-off in the sub-threshold region.

Averaging response over several devices in order to ameliorate observed differences in coupling efficiency, we estimate NFET responsivity to be in the range of 1V/W. The PFET responsivity is seen to be 20% that of the NFET, which is in agreement with the model predictions. Responsivities at 0.2THz and 0.6THz are found to be comparable, also consistent with the model. While the general form of the 1.6 THz response closely follows expectations, responsivities are significantly lower than expectations. The $R_g C_{gs}$ time constant for

these devices is estimated to be on the order of 0.2ps, which will attenuate response at 1.6 THz, and the inductance and the effective resistance of the bond wires due to the skin effect may also play a role at this frequency.

C. Drain current response enhancement

The affect of non-zero drain current on terahertz response was first reported by Lu and Shur.[9] They explain that biasing the detecting device into saturation decreases the value of the gate to drain capacitance, while increasing the gate to source capacitance, dramatically increasing the plasma wave boundary condition asymmetry, and thus enhancing the detector response. Veksler, et al.,[10] attribute the response enhancement to the increasing asymmetry of the field distribution with current leading to enhancement of the radiation induced potential at the drain side of the channel, and describe the detector response for long samples as follows:

$$\Delta v = \frac{v_d^2}{4V_{gs}} \frac{1}{\sqrt{1-\lambda}} \quad (4)$$

Here λ is the ratio of the drain current density to the saturation current density j_d/j_{dsat} . As the drain current approaches the saturation current, $\lambda \rightarrow 1$, and the detector response increases dramatically.

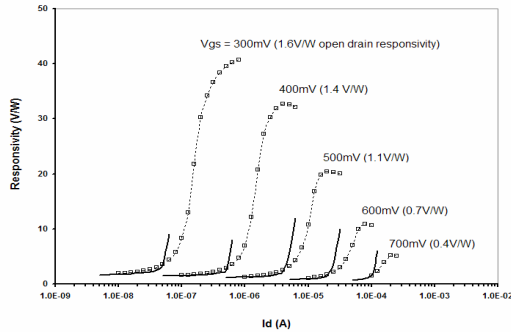


Figure 3. 0.2 THz responsivity of 2um x 60nm HVt NFET vs. drain current for selected gate bias values. The values in parentheses are the open drain responsivity measured for this device. Heavy lines illustrate the onset of response enhancement predicted by Eq. 4.

Response was measured in a similar fashion as in the open drain case, excepting that a high impedance current source was connected to the drain terminal in parallel with the preamplifier. Fig. 2 shows enhanced responsivity of a 2um x 60nm NFET at 0.2 THz, typical of our results. Both NFETs and PFETs showed a gate voltage dependent enhancement ranging from 10 to 25 times the open drain response at 0.2 THz and 0.6 THz. (1.6THz measurements are pending fixture improvements).

III. NOISE MEASUREMENTS

While responsivity represents the strength of detector output relative to the power of the input signal, equally important is the detectivity, describing the minimum signal which can be distinguished from ambient noise. A widely used measure is Noise Equivalent Power (NEP) which is inverse to the detectivity and is defined: “At a given data-signaling rate or modulation frequency, operating wavelength, and effective noise bandwidth, the radiant power that produces a signal-to-noise ratio of unity at the output of a given optical detector.” (from United States Federal Standard 1037C, entitled Telecommunications: Glossary of Telecommunication Terms). Commonly, NEP is considered to be the minimum power detectable per square root of bandwidth, in units of W/ $\sqrt{\text{Hz}}$. We calculate NEP as the inverse ratio of responsivity to the square root of measured device voltage noise.

A. Open drain noise

With $I_d = 0$, FET noise may be represented by the thermal voltage noise of the channel resistance: $S_V = 4k_B T R_{ch}$. Noise spectra were measured at several points near the device threshold using a quiet (battery/potentiometer) circuit for the gate bias. The source terminal was grounded and the drain connected to a spectrum analyzer with 1Mohm input impedance. Measured values were slightly higher than expected, likely due to electromagnetic stray and the non-unity noise figure of the amplifier used in measurements.

Noise and response measurements can also be performed concurrently[11] allowing direct calculation of NEP. Using this technique, we calculated NFET values of 6.5×10^{-8} W/ $\sqrt{\text{Hz}}$ and 1.6×10^{-8} W/ $\sqrt{\text{Hz}}$ at $V_{gs} = 300$ and 550mV respectively. Thus the detectivity maximum is found near the device threshold, rather than at the responsivity maximum, consistent with previous work.[8, 11] Compared with an NFET detector of equal dimensions, PFET NEP will be degraded by 1.5 times due to increased thermal noise in the higher resistance channel, and an additional 5 times due to lower responsivity.

B. Drain current noise

While introducing drain current into the detector can substantially increase the responsivity, as well there is a penalty in increased device noise. Noise spectra were measured at a variety of gate bias and drain currents adjusted such that the device is operated in transition between the linear and saturation regions where the response rises sharply. Gate and drain bias were adjusted as was the gate bias in the open drain measurements, with the drain connected through a 5.1 kohm load resistor. At low frequencies, the improvement in responsivity observed is completely overtaken by the large increase in device noise. At 100Hz, NEP at $V_{gs} = 300\text{mV}$ is 2.5×10^{-7} W/ $\sqrt{\text{Hz}}$, almost four times that of the open drain NEP, despite a 25 times greater responsivity. At response modulation frequencies in the range of 0.2 to 0.4GHz, the device noise is on par with that of the open drain configuration, and the drain current induced

responsivity increase becomes effective. At 0.4GHz and $V_{gs} = 500\text{mV}$, NEP reaches $4.5 \times 10^{-10} \text{ W}/\sqrt{\text{Hz}}$.

IV. RESPONSE SPEED

Detector response speed is fundamentally relevant in sensing applications involving substantial image processing, and in addition, has direct bearing on detectivity when the device is operated with drain current response enhancement. Kachorovskii and Shur have recently proposed theoretical calculation of the maximum response modulation frequency as shown in the following expression[12].

$$f_{\max} = \begin{cases} \frac{\mu V_{gt}}{2\pi L^2} & V_{gt} > 0, qV_{gt} \gg T \\ \frac{\mu \eta k_B T}{2\pi q L^2} & V_{gt} < 0, q|V_{gt}| \gg T \end{cases} \quad (5)$$

For our devices, using an average extracted NFET mobility of $100\text{cm}^2/\text{Vs}$, $f_{\max} = 40\text{GHz}$ at the device threshold, and 30GHz at the response maximum (typically $V_{gt} = -0.25\text{V}$).

V. CONCLUSIONS

We have demonstrated broadband terahertz and sub-terahertz response in both n-channel and p-channel silicon CMOS devices, and estimated responsivity and detectivity values for a range of device geometries. In general, shorter and wider devices increase both responsivity and detectivity as a result of reducing the channel resistance. In open drain configurations, maximum device detectivity for both device types is found to coincide with the threshold voltage, consistent with earlier NFET results. While responsivity is enhanced with the introduction of drain current, realizing improvements in detectivity require operation at near gigahertz frequencies, which we have demonstrated is possible by estimating maximum response modulation frequencies on the order of 10s of gigahertz.

Acknowledgements

The work of W. Stillman and D. Veksler was supported by the NSF (Grant No. 0333314) and by the NSF Connection One I/UCRC at RPI. The work was also partially supported by the RFBR (Grant 05-02-1772) and Civilian Research and Development Foundation (CRDF 2681).

VI. REFERENCES

[1] A. Steegen, R. Mo, R. Mann, M. C. Sun, M. Eller, G. Leake, D. Vietzke, A. Tilke, F. Guarin, A. Fischer, T. Pompl, G. Massey, A. Vayshenker, W. L. Tan, A. Ebert, W. Lin, W. Gao, J. Lian, J. P. Kim, P. Wrschka, J. H. Yang, A. Ajmera, R. Knoefler, Y.

W. Teh, F. Jamin, J. E. Park, K. Hooper, C. Griffin, P. Nguyen, V. Klee, V. Ku, C. Baiocco, G. Johnson, L. Tai, J. Benedict, S. Scheer, H. Zhuang, V. Ramachandran, G. Matusiewicz, Y. H. Lin, Y. K. Siew, F. Zhang, L. S. Leong, S. L. Liew, K. C. Park, K. W. Lee, D. H. Hong, S. M. Choi, E. Kaltalioglu, S. O. Kim, M. Naujok, M. Sherony, A. Cowley, A. Thomas, J. Sudijohno, T. Schiml, J. H. Ku, and I. Yang, "65nm CMOS technology for low power applications," Washington, DC, USA, 2005.

[2] M. I. Dyakonov and M. S. Shur, "Plasma wave electronics: Novel terahertz devices using two dimensional electron fluid," IEEE Transactions on Electron Devices, vol. 43, pp. 1640-1645, 1996.

[3] W. Knap, V. Kachorovskii, Y. Deng, S. Rumyantsev, J. Q. Lu, R. Gaska, M. S. Shur, G. Simin, X. Hu, M. Asif Khan, C. A. Saylor, and L. C. Brunel, "Nonresonant detection of terahertz radiation in field effect transistors," Journal of Applied Physics, vol. 91, pp. 9346, 2002.

[4] W. Knap, F. Teppe, Y. Meziani, N. Dyakonova, J. Lusakowski, F. Boeuf, T. Skotnicki, D. Maude, S. Rumyantsev, and M. S. Shur, "Plasma wave detection of sub-terahertz and terahertz radiation by silicon field-effect transistors," Applied Physics Letters, vol. 85, pp. 675-677, 2004.

[5] F. Teppe, W. Knap, D. Veksler, M. S. Shur, A. P. Dmitriev, V. Y. Kachorovskii, and S. Rumyantsev, "Room-temperature plasma waves resonant detection of sub-terahertz radiation by nanometer field-effect transistor," Applied Physics Letters, vol. 87, pp. 052107, 2005.

[6] N. Pala, F. Teppe, D. Veksler, Y. Deng, M. S. Shur, and R. Gaska, "Nonresonant detection of terahertz radiation by silicon-on-insulator MOSFETs," Electronics Letters, vol. 41, pp. 447-449, 2005.

[7] M. Dyakonov and M. Shur, "Detection, mixing, and frequency multiplication of terahertz radiation by two-dimensional electronic fluid," IEEE Transactions on Electron Devices, vol. 43, pp. 380-387, 1996.

[8] W. Stillman, M. S. Shur, D. Veksler, S. Rumyantsev, and F. Guarin, "Device loading effects on nonresonant detection of terahertz radiation by silicon MOSFETs," Electronics Letters, vol. 43, pp. 422-423, 2007.

[9] J. Q. Lu and M. S. Shur, "Terahertz detection by high-electron-mobility transistor: Enhancement by drain bias," Applied Physics Letters, vol. 78, pp. 2587, 2001.

[10] D. Veksler, F. Teppe, A. P. Dmitriev, V. Y. Kachorovskii, W. Knap, and M. S. Shur, "Detection of terahertz radiation in gated two-dimensional structures governed by dc current," Physical Review B (Condensed Matter and Materials Physics), vol. 73, pp. 125328-1, 2006.

[11] R. Tauk, F. Teppe, S. Boubanga, D. Coquillat, W. Knap, Y. M. Meziani, C. Gallon, F. Boeuf, T. Skotnicki, C. Fenouillet-Beranger, D. K. Maude, S. Rumyantsev, and M. S. Shur, "Plasma wave detection of terahertz radiation by silicon field effects transistors: Responsivity and noise equivalent power," Applied Physics Letters, vol. 89, pp. 253511, 2006.

[12] V. Y. Kachorovskii and M. S. Shur, "Field effect transistor as ultrafast detector of modulated terahertz radiation," Solid-State Electronics, Submitted for publication.